Optofluidics
Reserach Article • DOI: 10.2478/optof-2013-0002 • Optofluidics • 2013 • 11-18

VERSITA

In-line characterization and identification of micro-droplets on-chip

Abstract

We present an integrated optofluidic sensor system for in-line characterization of micro-droplets. The device provides information about the droplet generation frequency, the droplet volume, and the content of the droplet. Due to its simplicity this principle can easily be implemented with other microfluidic components on one and the same device. The sensor is based on total internal reflection phenomena. Droplets are pushed through a microfluidic channel which is hit by slightly diverging monochromatic light. At the solid-liquid interface parts of the rays experience total internal reflection while another part is transmitted. The ratio of reflected to transmitted light depends on the refractive index of the solution. Both signals are recorded simultaneously and provide a very stable output signal for the droplet characterization.
With the proposed system passing droplets were counted up to 320 droplets per second and droplets with different volumes could be discriminated. In a final experiment droplets with different amounts of dissolved $CaCl_2$ were distinguished based on their reflected and transmitted light pattern. This principle can be applied for the detection of any molecules in micro-droplets which significantly influence the refractive index of the buffer solution.

Keywords

micro droplets • partial total internal reflection • refractive index • optofluidics

PACS:

© Versita sp. z o.o.

Emanuel Weber[1*], Dietmar Puchberger-Enengl[2], Franz Keplinger[2], Michael J. Vellekoop[1†]

1 *Institute for Microsensors, -actuators, and -systems (IMSAS), MCB, University of Bremen Otto-Hahn-Allee, Build. NW1, 28359 Bremen, Germany*

2 *Institute of Sensor and Actuator Systems (ISAS), Vienna University of Technology Gusshausstrasse 27-29, 1040 Vienna, Austria*

Received 2013-04-08
Accepted 2013-04-26

1. Introduction

In the last decades microfluidics has shown its capability of manipulating liquids on the microscale for various applications. Especially biological and medical analysis systems benefit from its novel possibilities [1, 2]. One limitation for applications in these disciplines often is the available sample volume. Small amounts should be sufficient for the analysis. As a new subfield of microfluidics, micro-droplets enable the formation of encapsulated environments with volumes in the range of pico-liters [3, 4]. Two or more immiscible fluids [5] are brought into the same channel and allow the controlled appearance of emulsions on-chip. Recent works have demonstrated manipulation of micro-droplets through microfluidic channel systems [6–9]. Zagnoni *et al.* [10] have shown coalescence of distinct droplets which facilitates fully controlled reactions on-chip. Investigated applications of micro-droplets include chemical and biochemical screening [11, 12], enzymatic assays [13], and single cell encapsulation [14, 15].

The monitoring of micro-droplets is as important as their generation and manipulation. Information about the volume and the content of the droplets allow one to accurately observe and detect changes during the performed experiments, such as cell growth or chemical reactions. Therefore, reliable and fast in-line characterization methods are required. For the analysis of particles and cells microflow cytometry is a promising approach for high-throughput screening [16, 17]. Fattaccioli *et al.* [18] utilized a benchtop flow cytometer which also allows the analysis of micro-droplets. Nevertheless, for systems dealing with micro-droplets the monitoring is mostly

*E-mail: eweber@imsas.uni-bremen.de
†E-mail: mvellekoop@imsas.uni-bremen.de

Unangemeldet
Heruntergeladen am | 03.01.15 14:58

performed using conventional light microscopes requiring bulky and expensive equipment. Different approaches have already been followed to realize integrated read-out systems. One approach employs a capacity sensor allowing on-chip detection and control of droplets [19]. Srisa-Art *et al.* [20] used an external optical setup for the detection of single DNA molecules based on fluorescent labeling. In other works, an optical interrogation point has been directly integrated on-chip [21, 22]. In those works, the optical path is arranged perpendicular to the microfluidic channel. If droplets are passing this channel, the curvatures on both sides of the droplets result in light deflections which are detected in the signal recorded by an external avalanche photodiode. Droplets were analyzed with a throughput of 2.5 Hz. In that setup there is no information gathered while the body of elongated droplets is passing the interrogation point. The height of the peaks in the signal is solely dependent on the radii of the droplet curvatures which, on the other hand, is dependent on the contact angles of the employed liquids and the device material. Contact angles close to 90° could be critical for that principle. On the device presented by Shen *et al.* [23] a collimated light beam is directed towards a microfluidic channel. The reflected light signal is subsequently detected and used to derive information about the droplet size and content. In other works changes in the refractive index have been exploited for the realization of on-chip light switches [24, 25].

In this work an optofluidic sensor device is presented which exploits total internal reflection phenomena at the solid-liquid interface to characterize droplets in a microchannel. A similar arrangement has recently been used by Weber *et al.* to determine liquid concentrations [26, 27]. Fig. 1 illustrates the operation principle (adapted from [28]). Light is coupled into the device from an external light source. The center incident angle of the slightly diverging light beam on-chip is set close to the critical angle for total internal reflection. Due to the intentionally defined divergent incident light, some rays experience total internal reflection, while others are transmitted. The ratio of reflected to transmitted signals depends on the refractive index of the solution in the channel. In case of aqueous micro-droplets flowing through the device the refractive index of the continuous phase is much higher than the refractive index of the droplet itself. This difference can clearly be identified by monitoring the reflected and the transmitted light signals. In contrast to the device presented by Shen *et al.* [23] the implementation of a second signal allows for an improved signal stability. Furthermore, the diverging laser beam enables a drastically increased working range of the sensor device. In Fig. 1a a droplet is placed right at the interrogation point

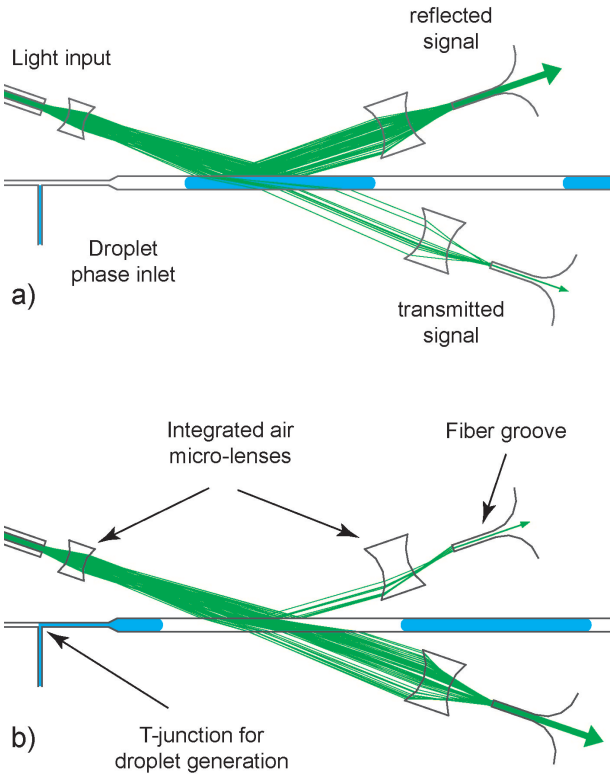

Fig 1. Schematic of the sensing principle. a) At aqueous droplets (low refractive index) the major part of the incident light experiences total internal reflection and results in a high reflected light signal. b) Between two droplets light passes through the continuous phase (high refractive index) and results in a high transmitted signal.

and results in a high reflected light signal. In Fig. 1b the light rays are passing between two droplets and produce a high transmitted signal. Using two signals for the read-out provides this sensing device with a high degree of stability. Furthermore, the system does not depend on contact angles and delivers information about the droplet throughout the entire time the droplet is passing the interrogation point. This principle does not only allow droplets to be detected but also to be characterized based on their refractive indices.

2. Materials

Dry film resist for device fabrication was purchased from ElgaEurope, Italy (Ordyl SY330 and SY317, n of approx. 1.52). Ordyl developer was composed of xylene, 2-butoxyethylester, and ethylbenzene (56/30/14, v/v/v; Sigma-Aldrich, USA). Mineral oil (n of 1.467, Sigma-Aldrich, USA) was used as continuous phase. A surfactant (1 % v/v, Span 80, n of 1.48; Sigma-Aldrich, USA)

Unangemeldet
Heruntergeladen am | 03.01.15 14:58

was added to increase the droplet stability [29]. For the droplet identification experiment calcium chloride dihydrate ($CaCl_2 2H_20$) was purchased from Carl Roth (Germany). A 531 nm diode pumped solid state laser (Optotronics, USA) was used as an external light source. Reduced cladding glass fibers (50 µm core diameter, 70 µm cladding diameter; Polymicro Technologies, USA) and pre-amplified silicon photodetectors (Thorlabs, USA) managed the peripheral setup. PC-controlled syringe pumps (cetoni GmbH, Germany) were used for the supply of droplet and continuous phase.

3. Device fabrication and design

For device fabrication a polyester foil was used as substrate. The microfluidic and optical elements were structured applying multiple layers of dry film resist. The total thickness of the applied resist and with that the height of the microfluidic and optical elements on-chip is 107 µm. The fabrication process for the devices was published by Weber *et al.* [28]. Similar fabrication protocols applying dry resists can be found in [27, 30, 31]. A photograph of the fabricated devices before cutting and bonding is illustrated in Fig. 2.

After development of the dry resist the devices are cut in size using conventional scissors. The independence from dicing machines allows any perimeters of the devices. Furthermore, the time for fabrication is kept at a minimum. Fig. 3a depicts a photograph of the final device bonded on a PMMA microscope slide. PTFE tubings manage the fluidic connections to the chip. In Fig. 3b and Fig. 3c scanning electron microscope images are given. The achieved resolution and aspect ratio facilitates application of this fabrication technology to microfluidic and optofluidic systems.

The center incident angle of the light beam is set to 19° with respect to the microfluidic channel. Therefore, the air micro-lens and the integrated waveguide at the light input region are rotated 19° clockwise from the horizontal. The incident angle and the dimensions of the micro-lenses were optimzed using ray-tracing simulations (ZEMAX, USA). For the optical part an excellent match of simulation and experimental data was obtained. The distance from the lens to the channel defines the size of the interrogation point and can be defined depending on the requirements. The collecting lens for the transmitted light signal is aligned in the same angle as the lens at the light input region. The second collecting lens for the reflected signal is rotated 19° counterclockwise from the horizontal. Both collecting lenses are placed as close to the microfluidic channel as possible to minimize light losses. The numerical apertures of the lens at the light input region and the two collecting lenses are 0.55 and

Fig 2. Photograph of fabricated devices before cutting and bonding. The microfluidic and optical elements are structured in dry resist. A polyester foil is used as substrate.

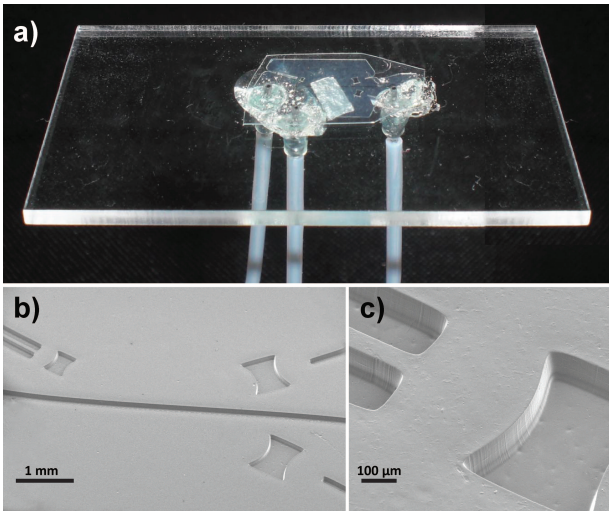

Fig 3. a) Photograph of a final device bonded on a PMMA microscope slide. The fluidic connections to the peripheral syringe pumps are managed by PTFE tubings. A highly reflective material (aluminum foil) is glued underneath the interrogation point to achieve higher optical contrast in the microscope images. Scanning electron microscope images of b) the optical interrogation point on-chip and c) a magnification of an integrated air micro-lens.

0.59, respectively. The optical elements on-chip can also be redesigned for other refractive indices. With that, the device can be optimized for nearly any droplet-continuous phase combination.

4. Experimental setup

The experimental setup, consisting of an external light source, reduced cladding glass fibers, two pre-amplified silicon photodetectors, a digital storage oscilloscope, a

Unangemeldet
Heruntergeladen am | 03.01.15 14:58

syringe pump, the continuous phase, the droplet phase, a fluidic waste box, and the optofluidic chip, is given in Fig. 4.

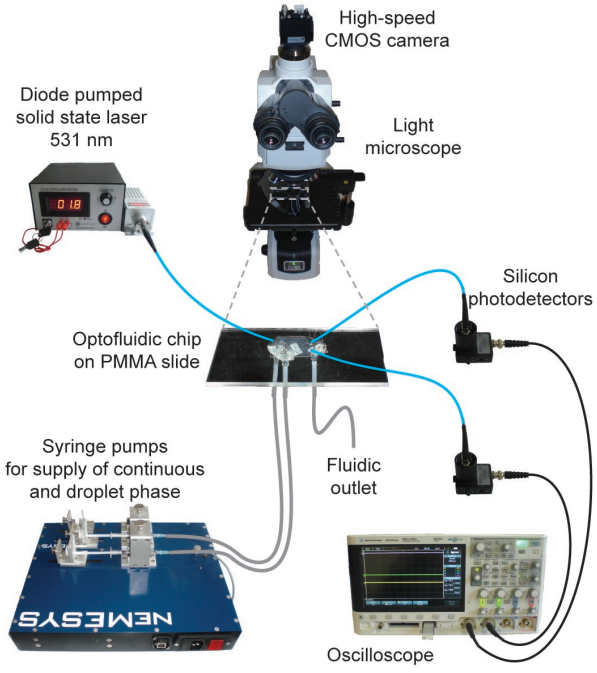

Fig 4. Experimental setup consisting of a light microscope, a high speed CMOS camera, an external light source, three reduced cladding glass fibers (blue lines), two pre-amplified silicon photodetectors, a digital storage oscilloscope, a syringe pump, the continuous phase, the droplet phase, a fluidic outlet, and the optofluidic chip.

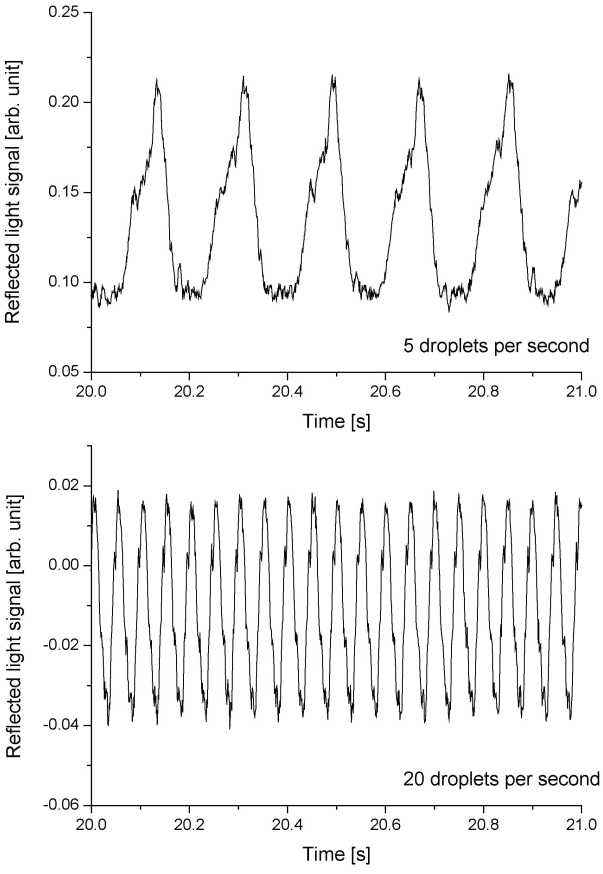

Fig 5. Signals recorded at the reflected output for two different droplet generation frequencies. Each peak in the signals represents a single droplet passing the interrogation point.

One side of the glass fibers is equipped with an SMA connector for direct connection to the light source and the photodetectors. The bare, other end is clamped onto the optofluidic chip using integrated fiber-grooves. The signals of the two photodetectors are recorded simultaneously using a digital storage oscilloscope. A PC-controlled syringe pump is used for the supply of continuous and droplet phase. Micro-droplets are generated using a T-junction on chip. For visual inspection of the micro-droplets the optofluidic chip is placed under a light microscope having a high-speed CMOS camera (up to 10,000 frames per second) attached.

5. Results and discussion

Because of the hydrophobicity of the device material the continuous phase, coating the channel walls, was mineral oil. The droplet phase was either DI water or an aqueous $CaCl_2$ solution. Applying other materials would allow the formation of oil in water droplets as well.

5.1. Detection of micro-droplets

Droplets passing the interrogation point result in changes in both the reflected and the transmitted light signals. Due to the low refractive index of the droplet the reflected light signal increases while the transmitted decreases simultaneously. Applying a peak-detection algorithm at either of those two signals allows the detection of single droplets. This peak-detection can be used to count droplets. In Fig. 5 signals recorded at the reflected output for two different droplet generation frequencies are shown.

Applying this procedure, droplets were successfully counted up to 320 droplets per second (Fig. 6). With increasing frequency the stability of the droplet generation decreases which explains the increased standard deviation in the diagram. Above a droplet generation frequency of 320 droplets per second the T-junction does not allow a stable formation of droplets anymore. At higher frequencies two streams of liquid, DI-water next to oil, are achieved rather than a break-up into individual

Unangemeldet
Heruntergeladen am | 03.01.15 14:58

droplets. Implementation of other droplet generation units (e.g. cross-junction) would solve this issue. The proposed analysis principle itself is not limited here and can be applied for higher droplet generation frequencies as well.

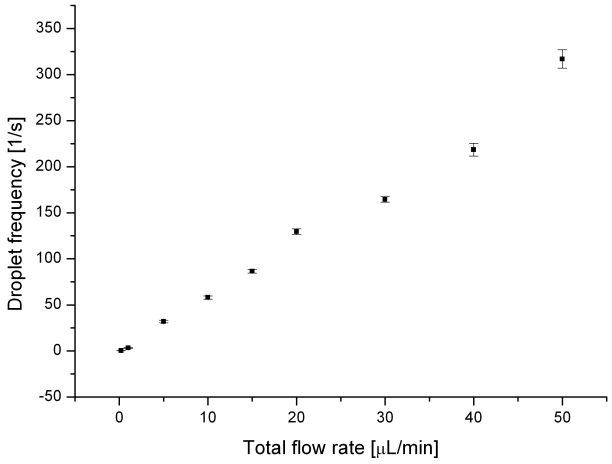

Fig 6. Droplet counting up to 320 droplets per second. A nearly linear relation between total flow rate and droplet frequency is obtained.

5.2. Sizing of micro-droplets

Droplets of different volume generate different peaks in the reflected and the transmitted signals. In Fig. 7 elongated droplets, squeezed inside the channel as well as small spherical droplets are depicted. The droplet volume was defined by alternating the flow velocities of droplet and continuous phase. The total flow rate was kept at 6 µL/min. For a univocal determination of the droplet volume the total flow rate has to be known. The implementation of a second optical sensor on the device would provide this information even for systems with fluctuating flow rates.

Both signals were examined separately. Each individual peak generated in the reflected signal by a passing droplet was integrated. The obtained values for all investigated droplet volumes are given in Fig. 8. For elongated droplets (I, II, and III) the reflected signal can be used for sizing. The obtained values are clearly separated. With decreasing droplet size the peaks in the reflected signal decrease proportionally. Once the droplet shape changes from elongated to spherical a univocal discrimination of the droplets cannot be provided anymore. The obtained values clearly overlap (IV and V).

For the transmitted signal the same procedure was applied. Each individual peak generated by a single droplet was integrated and plotted in Fig. 9. The behavior is the contrary compared to the analysis of the reflected signal. For elongated droplets (I, II, and III) no separation

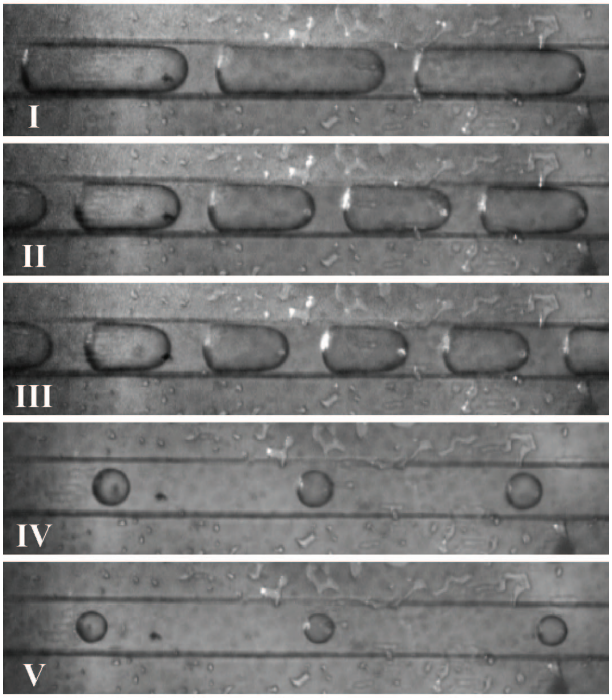

Fig 7. Micrographs of five droplet with different volumes. Elongated (I+II+III), as well as spherical droplets (IV+V) are shown. Depending on the droplet volume different peaks in the signals are obtained. The width of the microfluidic channel is 100 µm.

is possible. With decreasing droplet size the peaks in the transmitted signal increase. For spherical droplets (IV and V) a well-defined separation based on the droplet size is achieved. Exploiting the information obtained from both signals droplets can be sized over a huge range of dimensions. Elongated as well as spherical droplets can be examined on one and the same device.

5.3. Identification of micro-droplets

The height of the reflected and the transmitted signals depends on the refractive index of the droplet phase. This circumstance can be exploited for the identification of the droplet content. To investigate this capability of the device $CaCl_2$ solutions at different concentrations were sequentially used as droplet phase. For each concentration the peaks in the reflected and transmitted signals were again integrated individually. The corresponding values of reflected and transmitted peak integration were then subtracted for each droplet. The obtained results are given in Fig. 10. In this experiment the total flow rate was set to 1.5 µL/min (continuous phase: 0.5 µL/min; droplet phase: 1 µL/min). The resulting droplet generation frequency was approx. 4.5 droplets per second. For each $CaCl_2$ concentration about 100 micro-droplets were analyzed.

Unangemeldet
Heruntergeladen am | 03.01.15 14:58

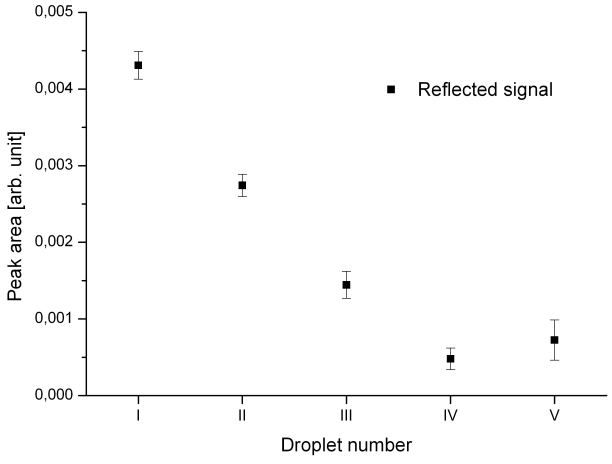

Fig 8. Peak integration applied on the reflected light signal for different droplet volumes. Elongated droplets (I, II, and III) can be discriminated. Spherical droplets not or hardly touching the channel walls result in a poor separation based on the reflected light signal (IV and V).

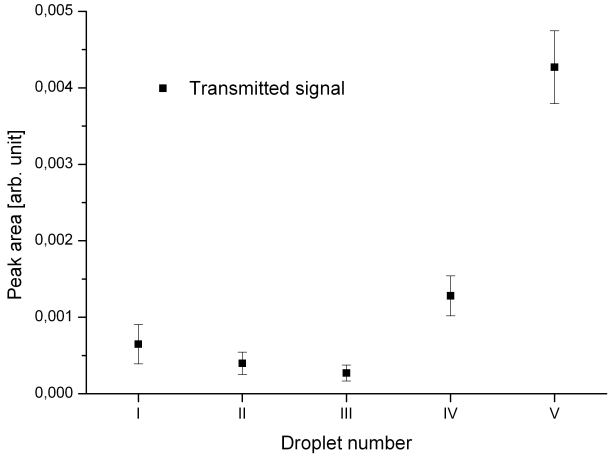

Fig 9. Peak integration applied on the transmitted light signal for different droplet volumes. Elongated droplets (I, II, and III) cannot be discriminated. Spherical droplets not or hardly touching the channel walls result in an excellent separation based on the transmitted light signal (IV and V).

With increasing $CaCl_2$ concentration the refractive index of the droplet increases [32]. At higher refractive indices the amount of transmitted light increases while the reflected signal decreases simultaneously. The results indicate highest sensitivity of the device at a $CaCl_2$ concentration of 5 M. In that region changes in the concentration of approx. 70 mM can be detected. The range of sensitivity can be optimized for other refractive indices by redesigning the optical elements. In that way, devices can be designed for various analytes as long as they influence the refractive index of the buffer solution. This sensor

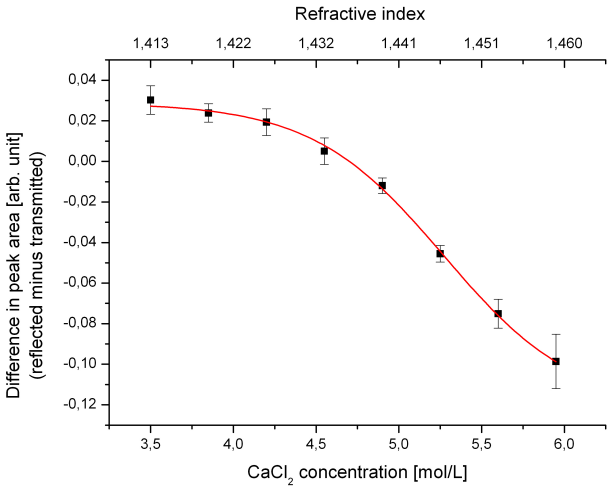

Fig 10. Difference in peak area of reflected and transmitted light signal for different $CaCl_2$ content in the droplets. The difference decreases with increasing refractive index meaning increasing $CaCl_2$ concentration. At approx. 5 M the device shows highest sensitivity. This range of sensitivity can be shifted by re-dimensioning of the optical elements on-chip.

principle can be applied to quantitatively detect changes in the amount of one certain molecule such as, for example, $CaCl_2$, either between two distinct droplets or in the same droplet at different time points. As those sensors are applied to known systems external physical parameters, such as absorbance, fluorescence, or light scattering effects, have only marginal impact on the results. Furthermore, the temperature stability of the entire system (changes of ± 1°C are not detectable in the signals) allows a robust application of the sensor device.

6. Conclusions

The proposed device proves suitable for an in-line characterization of micro-droplets. Having the interrogation point implemented on-chip the device can be operated in a plug-and-play mode. The light alignment is irreversibly defined on the device by the geometry. The sensor allows detection and counting of individual droplets. The limit of 320 droplets per second has arisen from the droplet generation principle. The actual limit of the analysis principle has not been reached so far. Furthermore, information on the droplet volume and size can be gathered in a flow-through manner. Taking the information of reflected and transmitted light signals elongated as well as spherical droplets can be sized on one and the same device.

Another novel feature of this device is its capability of identifying droplets based on their contents. Discrimination of droplets containing different amounts of dissolved $CaCl_2$ has been demonstrated. The range of sensitivity

Unangemeldet
Heruntergeladen am | 03.01.15 14:58

can be optimized for the given requirements. In that sense, the sensor can be applied for a range of applications. Examples are the monitoring of the glucose level and the ethanol content for biological experiments, the detection of phosphates in water studies, and the analysis of the DNA content in micro-droplets. Any molecules which have a significant impact on the refractive index can be detected applying this principle. Especially, the simplicity of the design allows integration with other microfluidic components on one and the same device to develop sophisticated lab-on-a-chip devices.

Acknowledgments

This project was financially supported by the European Marie Curie Initial Training Network *EngCaBra*; project number PITN-GA-2010-264417.

References

[1] G. M. Whitesides, "The origins and the future of microfluidics." *Nature*, vol. 442, no. 7101, pp. 368–373, Jul 2006.

[2] S. Haeberle, G. Roth, F. von Stetten, R. Zengerle *et al.*, "Microfluidic lab-on-a-chip platforms: requirements, characteristics and applications," *Chemical Society Reviews*, vol. 39, no. 3, pp. 1153–1182, 2010.

[3] A. Huebner, S. Sharma, M. Srisa-Art, F. Hollfelder, J. B. Edel, and A. J. deMello, "Microdroplets: A sea of applications?" *Lab on a Chip*, vol. 8, pp. 1244–1254, 2008.

[4] X. C. i. Solvas and A. deMello, "Droplet microfluidics: Recent developments and future applications." *Chemical Communications*, vol. 47, pp. 1936–1942, 2011.

[5] S. Hardt and T. Hahn, "Microfluidics with aqueous two-phase systems." *Lab on a Chip*, vol. 12, pp. 434–442, 2012.

[6] S. S. Bithi and S. A. Vanapalli, "Behavior of a train of droplets in a fluidic network with hydrodynamic traps." *Biomicrofluidics*, vol. 4, p. 044110, 2010.

[7] M. Abdelgawad and A. R. Wheeler, "The digital revolution: A new paradigm for microfluidics." *Advanced Materials (Weinheim, Germany)*, vol. 21, pp. 920–925, 2009.

[8] L. Malic, D. Brassard, T. Veres, and M. Tabrizian, "Integration and detection of biochemical assays in digital microfluidic LOC devices." *Lab on a Chip*, vol. 10, pp. 418–431, 2010.

[9] Z. Wang and J. Zhe, "Recent advances in particle and droplet manipulation for lab-on-a-chip devices based on surface acoustic waves." *Lab on a Chip*, vol. 7, pp. 1280–1285, 2011.

[10] M. Zagnoni and J. M. Cooper, "On-chip electrocoalescence of microdroplets as a function of voltage, frequency and droplet size." *Lab on a Chip*, vol. 9, pp. 2652–2658, 2009.

[11] H. Song, M. R. Bringer, J. D. Tice, C. J. Gerdts, and R. F. Ismagilov, "Experimental test of scaling of mixing by chaotic advection in droplets moving through microfluidic channels," *Applied Physics Letters*, vol. 83, no. 22, pp. 4664–4666, 2003.

[12] H. Song, J. D. Tice, and R. F. Ismagilov, "A microfluidic system for controlling reaction networks in time." *Angewandte Chemie International Edition*, vol. 42, pp. 768–772, 2003.

[13] H. Song and R. F. Ismagilov, "Millisecond kinetics on a microfluidic chip using nanoliters of reagent." *Journal of the American Chemical Society*, vol. 125, pp. 14 613–14 619, 2003.

[14] J. F. Edd, D. Di Carlo, K. J. Humphry, S. Köster, D. Irimia, D. A. Weitz, and M. Toner, "Controlled encapsulation of single-cells into monodisperse picolitre drops." *Lab on a Chip*, vol. 8, pp. 1262–1264, 2008.

[15] T. Konry, M. Dominguez-Villar, C. Baecher-Allan, D. A. Hafler, and M. L. Yarmush, "Droplet-based microfluidic platforms for single t cell secretion analysis of IL-10 cytokine." *Biosensors and Bioelectronics*, vol. 26, pp. 2707–2710, 2011.

[16] M. Rosenauer, W. Buchegger, I. Finoulst, P. Verhaert, and M. Vellekoop, "Miniaturized flow cytometer with 3d hydrodynamic particle focusing and integrated optical elements applying silicon photodiodes." *Microfluidics and Nanofluidics*, vol. 10, no. 4, pp. 761–771, Oct. 2010.

[17] E. Weber, M. Rosenauer, W. Buchegger, P. D. E. M. Verhaert, and M. J. Vellekoop, "Fluorescence based on-chip cell analysis applying standard viability kits." in *Proc. of the microTAS 2011*, Seattle, USA, 2011, pp. 1716–1718.

[18] J. Fattaccioli, J. Baudry, J.-D. Émerard, E. Bertrand, C. Goubault, N. Henry, and J. Bibette, "Size and fluorescence measurements of individual droplets by flow cytometry." *Soft Matter*, vol. 11, pp. 2232–2238, 2009.

[19] X. Niu, M. Zhang, S. Peng, W. Wen, and P. Sheng, "Real-time detection, control, and sorting of microfluidic droplets." *Biomicrofluidics*, vol. 1, p. 044101, 2007.

[20] M. Srisa-Art, A. J. deMello, and J. B. Edel, "High-throughput confinement and detection of single DNA molecules in aqueous microdroplets." *Chemical Communications*, vol. 43, pp. 6548–6550, 2009.

[21] N.-T. Nguyen, S. Lassemono, and F. A. Chollet, "Optical detection for droplet size control in microfluidic

Unangemeldet
Heruntergeladen am | 03.01.15 14:58

droplet-based analysis systems." *Sensors and Actuators B: Chemical*, vol. 117, pp. 431–436, 2006.

[22] N.-T. Nguyen, S. Lassemono, F. A. Chollet, and C. Yang, "Interfacial tension measurement with an optofluidic sensor." *IEEE Sensors Journal*, vol. 7, no. 5, pp. 692–697, 2007.

[23] Z. Shen, Y. Zou, and X. Chen, "Characterization of microdroplets using optofluidic signals." *Lab Chip*, vol. 12, no. 19, pp. 3816–3820, Aug 2012.

[24] E. Weber, F. Keplinger, and M. J. Vellekoop, "Optofluidic, contact-free 1x3 light-switch fabricated on a mono-layer device," in *Proceedings of the 3rd European Conference on Microfluidics*, Heidelberg, Germany, 2012.

[25] K. Campbell, A. Groisman, U. Levy, L. Pang, S. Mookherjea, D. Psaltis, and Y. Fainman, "A microfluidic 2x2 optical switch." *Applied Physics Letters*, vol. 85, no. 25, pp. 6119–6121, 2004.

[26] E. Weber and M. J. Vellekoop, "Optofluidic microsensors for the determination of liquid concentrations." *Lab on a Chip*, vol. 12, no. 19, pp. 3754–3759, Aug 2012.

[27] E. Weber, F. Keplinger, and M. Vellekoop, "Detection of dissolved lactose employing an optofluidic microsystem," *Diagnostics*, vol. 2, no. 4, pp. 97–106, 2012.

[28] E. Weber, D. Puchberger-Enengl, and M. J. Vellekoop, "In-line characterization of micro-droplets based on partial light reflection at the solid-liquid interface." in *Proc. of the ASME 2012 10th ICNMM*, Puerto Rico, USA, 2012, p. To be published.

[29] J.-C. Baret, "Surfactants in droplet-based microfluidics." *Lab on a Chip*, vol. 12, no. 3, pp. 422–433, Feb 2012.

[30] P. Vulto, N. Glade, L. Altomare, J. Bablet, L. D. Tin, G. Medoro, I. Chartier, N. Manaresi, M. Tartagni, and R. Guerrieri, "Microfluidic channel fabrication in dry film resist for production and prototyping of hybrid chips." *Lab on a Chip*, vol. 5, no. 2, pp. 158–162, Feb 2005.

[31] D. Puchberger-Enengl, S. Podszun, H. Heinz, C. Hermann, P. Vulto, and G. A. Urban, "Microfluidic concentration of bacteria by on-chip electrophoresis." *Biomicrofluidics*, vol. 5, no. 4, pp. 44 111–4 411 110, Dec 2011.

[32] D. Lide, *CRC Handbook of Chemistry and Physics*, 88th ed., P. J. Mohr and B. N. Taylor, Eds. Boca Raton, 2007.

Unangemeldet
Heruntergeladen am | 03.01.15 14:58